Dynamic polarizability, Cauchy moments, and the optical absorption spectrum of liquid water: A sequential molecular dynamics/quantum mechanical approach

Ricardo A. Mata,[1] Benedito J. Costa Cabral,[1,2,a)] Claude Millot,[3] Kaline Coutinho,[4] and Sylvio Canuto[4]

[1]*Grupo de Física Matemática, Universidade de Lisboa, Av. Professor Gama Pinto 2, 1649-003 Lisboa, Portugal*

[2]*Departamento de Química e Bioquímica, Faculdade de Ciências, Universidade de Lisboa, 1749-016 Lisboa, Portugal*

[3]*Équipe Chimie and Biochimie Théorique, UMR CNRS-UHP 7565, Université Henri Poincaré, F-54506 Vandoeuvre-lés-Nancy Cedex, France*

[4]*Instituto de Física, Universidade de São Paulo, CP 66318, 05315-970 São Paulo, Brazil*

(Received 3 September 2008; accepted 29 November 2008; published online 6 January 2009; publisher error corrected 7 January 2009)

The dynamic polarizability and optical absorption spectrum of liquid water in the 6–15 eV energy range are investigated by a sequential molecular dynamics (MD)/quantum mechanical approach. The MD simulations are based on a polarizable model for liquid water. Calculation of electronic properties relies on time-dependent density functional and equation-of-motion coupled-cluster theories. Results for the dynamic polarizability, Cauchy moments, $S(-2)$, $S(-4)$, $S(-6)$, and dielectric properties of liquid water are reported. The theoretical predictions for the optical absorption spectrum of liquid water are in good agreement with experimental information. © *2009 American Institute of Physics*. [DOI: 10.1063/1.3054184]

I. INTRODUCTION

The interaction of radiation with water controls the dynamics of chemical and biochemical processes of central importance for life. Therefore water photophysics/photochemistry deserved the attention of several works in the scientific literature.[1–12] One specific and central issue concerns the absorption spectrum of water over a wide energy range. The water molecule is characterized by absorption of radiation in the infrared and ultraviolet (UV) regions. This is also observed in liquid water although some features related to the formation of a complex hydrogen bonding (HB) network are specific of the liquid phase and well known examples include the gas to liquid phase redshift of the O–H stretching frequency[13] and the blueshift of the first maximum of the optical absorption spectrum in the UV region.[8]

The strong interest on this subject motivated several theoretical studies on the electronic properties of water[14] with emphasis on the calculation of electronic excitations and molecular polarizabilities.[15–20] Recently, some theoretical studies were dedicated to the study of the optical absorption and dielectric properties of liquid water.[21–24] In spite of the relative success of these theoretical studies some important questions persist. In particular the absorption spectrum of water in the high-energy side and the role of HB on line broadening deserve more attention. Moreover, reliable theoretical approaches for the prediction of water electronic properties are useful for investigating the absorption spectra and dielectric properties of confined[25,26] and supercritical water,[27] which are much less understood.

In this work, we report a sequential molecular dynamics (MD)/quantum mechanical (QM) study of the absorption spectrum of liquid water in the 6–15 eV energy range. The MD simulations are based on a polarizable model of liquid water.[28] The *a posteriori* QM calculations of its electronic properties rely on time-dependent density functional theory (TDDFT) (Ref. 29) and equation-of-motion coupled-cluster with single and double excitations (EOM-CCSD).[30] Emphasis is placed on the calculation of the dynamic polarizability, Cauchy moments, and dielectric properties of liquid water. Initially, details on the adopted theoretical methodology and comparison between TDDFT, EOM-CCSD, and experimental data for excitation energies of the water molecule are reported. Then, results for the dynamic polarizability, Cauchy moments, and dielectric properties are compared with theoretical predictions and experimental data. A discussion on the relationship between HB formation and the absorption spectrum of liquid water is also presented.

II. COMPUTATIONAL DETAILS

The MD simulation has been carried out in the (*NVE*) microcanonical ensemble with the Niesar–Corongiu–Clementi (NCC) model[28] for polarizable water with $N=343$ molecules in a cubic box with periodic boundary conditions at a density $\rho=0.997$ g cm^{-3} and average temperature T

a)Author to whom correspondence should be addressed. Electronic mail: ben@cii.fc.ul.pt.

=298 K. The NCC geometry for the water molecule is the experimental gas phase structure (O–H=0.9572 Å, HOH =104.52°).

A detailed description of the polarizable NCC model as well as results for the structure and dynamics of water predicted by this model can be found in the work by Niesar *et al.*[28] A sequential MD/QM study of liquid water based on the NCC model was recently reported.[31] In the sequential MD/QM approach, a series of configurations generated by integration of the equations of motion is used for *a posteriori* calculations of the electronic properties. Of particular importance in performing sequential MD/QM calculations are the structure of the system and the charge distribution of the molecules (if the quantum calculations are carried out in an embedded quantum system). Therefore, it is important to assess the quality of the structure generated by the NCC model as well as the adequacy of the embedding charge distribution for describing polarization effects in liquid phase. The pair correlation functions for O–O, O–H, and H–H correlations predicted by the NCC model (see Fig. 3 of Niesar *et al.*[28]) are in good agreement with the experimental information.[32–34] Integration of the O–O pair correlation function up to the first minimum (3.3) leads to 4.3, which is the average number of water molecules in the first coordination shell. Dielectric properties of the NCC model were investigated by Soetens *et al.*[35] Specifically, the static dielectric constant of the polarizable NCC model (100±8) (Ref. 35) is in acceptable agreement with the experimental value for liquid water (78). Therefore, it seems reasonable to assume that the present model can correctly describe both the structure and polarization effects in liquid water.

100 configurations (saved every 20 ps) were selected for the calculation of the electronic properties. Successive configurations generated by MD or Monte Carlo simulations are strongly correlated and when the property of interest involves a high computational effort, the use of uncorrelated structures is of crucial importance for evaluating averages over a relatively small number of representative configurations.[36] Each configuration includes a quantum system with one to three water molecules ($N_w=1-3$), which are embedded in the charge distribution of the closest 100 surrounding water molecules. Thus, for the electronic structure calculations, three different systems were defined: $N_w=1+100$, $2+100$, $3+100$, which correspond, respectively, to one, two, and three explicit water molecules (the quantum system), embedded in 100 water molecules represented as point charges. In order to investigate how the results depend on the size of the quantum system, calculations with four and five explicit water molecules ($N_w=4+100$ and $N_w=5+100$) are also reported. The charge distribution of the embedding molecules is represented by the permanent charges of the NCC model as well as by the charges representing the induced dipole moments on each O–H bond of the water molecule. For the QM calculations, the self-consistent induced dipole moments associated with the local O–H bond polarizability were reproduced by placing two point charges of ±0.2 a.u., separated by a variable vector, which is centered on the O–H bond at a distance of 0.432 96 Å from the oxygen atom. The embedding charges mimic the presence of the surrounding water molecules and no periodic boundary conditions were applied for predicting electronic properties.

TDDFT calculations were carried out with the hybrid BHandHLYP functional, which is based on the combination of the Hartree–Fock and Becke88 (Ref. 37) functional for exchange, and the Lee–Yang–Parr (LYP) functional for correlation.[38] The BHandHLYP functional as implemented in the GAUSSIAN 03 suite of programs[39] is defined as $0.5E_x^{\mathrm{HF}}+0.5E_x^{\mathrm{LSDA}}+0.5\Delta E_x^{\mathrm{Becke88}}+E_c^{\mathrm{LYP}}$. Some calculations with the hybrid PBE0 functional[40] based on the Perdew–Burke–Ernzerhof (PBE) exchange-correlation functional[41] are also reported. EOM-CCSD (Ref. 30) calculations were carried out with a development version of the MOLPRO 2006.4 package.[42] The Dunning's double augmented correlation-consistent basis sets (d-aug-cc-pVxZ; $x=D$, T, Q)[43] were used for the gas and liquid phases calculations (we will adopt dapvxz for representing these basis sets).

The calculation of the complex dynamic polarizability $\alpha(\omega)=\alpha_1(\omega)+i\alpha_2(\omega)$, where $\alpha_1(\omega)$ and $\alpha_2(\omega)$ are the real and imaginary parts of $\alpha(\omega)$, was carried out through a sum-over-states (SOS) according to the following expression:[44]

$$\alpha(\omega)=\sum_{k=0}^{\infty} f_k\left\{\frac{\Delta E_k^2-\omega^2}{(\Delta E_k^2-\omega^2)^2+\omega^2\Gamma_k^2}+\frac{i\Gamma_k\omega}{(\Delta E_k^2-\omega^2)^2+\omega^2\Gamma_k^2}\right\}, \tag{1}$$

where ΔE_k and f_k are transition energies and oscillator strengths, respectively, and $1/\Gamma_k$ is a decay time describing the radiative relaxation of transition k. Γ_k can be estimated as $\Gamma_k=\hbar/\tau=6.582\times10^{-16}$ eV s/τ, where the decay time is on the femtosecond timescale.[45] Γ_k has been set to a single arbitrary and small value (0.5442 eV or 0.02 a.u.).

The convergence of the SOS for evaluating polarizabilities will be discussed in the next section. Finite-field (FF) calculations of the gas phase dynamic polarizability are also reported. The number of excited states (N_{states}) included in TDDFT corresponds to the number of single excitations from the ground state, i.e., $N_{\mathrm{states}}=N_{\mathrm{occupied}}N_{\mathrm{virtual}}$. For $N_w=1+100$, N_{states} are 265 (dapvdz), 605 (dapvtz), and 1120 (dapvqz). For $N_w=2+100$ and $N_w=3+100$ the calculations were performed with the dapvdz basis set and N_{states} are, 1060 and 2385, respectively. Calculations for $N_w=4+100$ and $N_w=5+100$ were also performed. However, in these cases, smaller basis sets were used: cc-pVDZ (H atoms) and aug-cc-pVDZ (O atoms). Moreover, for $N_w=5+100$ the SOS was truncated at 500 states. Core excitations were not included in EOM-CCSD calculations and $N_{\mathrm{states}}=250$ for $N_w=1+100$ and dapvdz basis set.

For small frequencies, $\alpha_1(\omega)$ can be represented by the following series:

$$\alpha_1(\omega)=\sum_{j=0}^{\infty} S(-2j-2)\omega^{2j}, \tag{2}$$

where ω is the frequency and $S(j)$ are known as the Cauchy moments.[46,47] We will assume that in the low-energy regime $\alpha_1(\omega)$ is given by[47]

TABLE I. Lowest excitation energies (ω in eV) from the ground state ($1\ ^1A_1$)and oscillator strengths (f in a.u.) of the gas phase water molecule [Theoretical calculations with the d-aug-cc-pVTZ basis-set and NCC geometry for the water molecule (OH=0.9572 Å and HOH=104.52°)].

State		BHandHLYP	PBE0	EOM-CCSD	Expt.[a]
			Valence excitations		
$1\ ^1B_1$	ω	7.68	7.18	7.61	7.5
	f	0.0445	0.0453	0.051	0.0497[b]
$1\ ^1A_2$	ω	9.25	8.54	9.36	9.1
$2\ ^1A_1$	ω	9.77	8.97	9.87	9.7
	f	0.0419	0.0035	0.0577	0.0732,[b]0.0509[c]
$2\ ^1B_1$	ω	9.82	8.87	10.00	10.0
	f	0.0061	0.0001	0.0082	0.0052[b]
$3\ ^1A_1$	ω	10.06	9.40	10.22	10.2
	f	0.0430	0.0730	0.0436	0.0460,[b]0.022[c]
$3\ ^1B_1$	ω	10.11	9.00	10.63	10.5
	f	0.0011	0.0055	0.0000	
$2\ ^1A_2$	ω	10.38	9.16	10.90	10.8
$^3B_1$	ω	7.19	6.76		7.1
$^3A_2$	ω	9.04	8.41		9.0
$^3A_1$	ω	9.27	8.75		9.3
			Core excitations		
$^1A_1$	ω	531.7	520.7		534.0
$^1B_2$	ω	533.1	522.1		535.9
$^1B_1$	ω	534.4	522.6		537.1

[a]See Ref. 48 and references therein.
[b]From Ref. 9.
[c]From Ref. 49.

$$\alpha_1(\omega) = S(-2) + S(-4)\omega^2 + S(-6)\omega^4, \quad (3)$$

where $S(-2)$ is the static polarizability $\alpha(0)$. These Cauchy moments are then obtained by a fitting of the $\alpha_1(\omega)$ curve for small values of ω.

III. RESULTS AND DISCUSSION

A. Dynamic polarizability and Cauchy moments

The lowest excitation energies for the gas phase water molecule are reported in Table I, where they are gathered with data from the literature.[9,48,49] Comprehensive discussions on the main features characterizing the electronic spectrum of the water molecule were previously reported.[15] Here, we would like to highlight the very good agreement between BHandHLYP, EOM-CCSD, and experimental results for the lowest excitation energies and oscillator strengths for the isolated water molecule. Moreover, for core excitations a good agreement between BHandHLYP and the experiment can also be observed. Excitation energies are clearly underestimated by PBE0 calculations. The performance of other approaches including *ab initio* methods and the Coulomb attenuated B3LYP functional (CAM-B3LYP) (Ref. 50) for predicting excitation energies of the isolated water molecule was investigated by Paterson *et al.*[51] For the water molecule the excitation energies calculated by using CAM-B3LYP (Ref. 51) and PBE0 (Table I) with the dapvtz basis set are quite similar. Therefore, unless otherwise stated, only TD-DFT results based on the BHandHLYP will be further analyzed.

The behavior of the static polarizability ($\alpha(0)$) with the number of states included in the SOS for the dapv$x$z ($x=D,T,Q$) basis sets is shown in Fig. 1. Very similar values for $\alpha(0)$ are predicted by the different basis sets. However, the number of states (N_{states}) necessary for obtaining convergence is clearly basis-set dependent. SOS, complex polarization propagator (PP) (Refs. 52 and 53), and FF results for the undamped dynamic polarizability [$\Gamma_k=0$ in Eq. (1) and $\alpha(\omega)=\alpha_1(\omega)$] in the 4–18 eV range are reported in Fig. 2 (top panel) for the water molecule in the gas phase. Calculations based on the PP approach were carried out with the DALTON program.[54] A very good agreement between the different procedures can be observed. Specifically, the energies

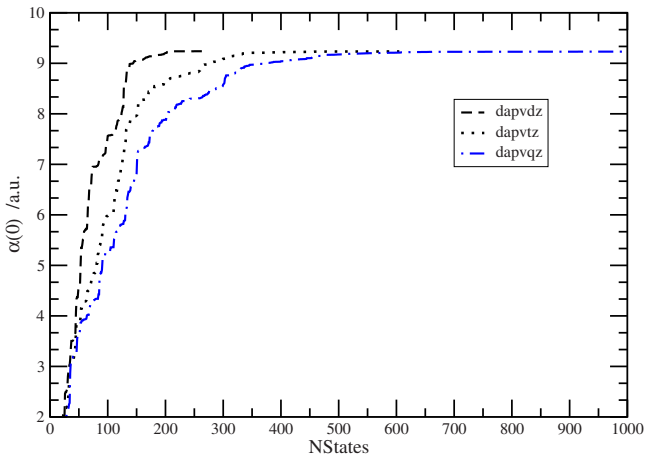

FIG. 1. (Color online) Dependence of the static polarizability of water with the basis-set and number of states (N_{states}) included in the SOS for dapvdz, dapvtz, and dapvqz basis sets.

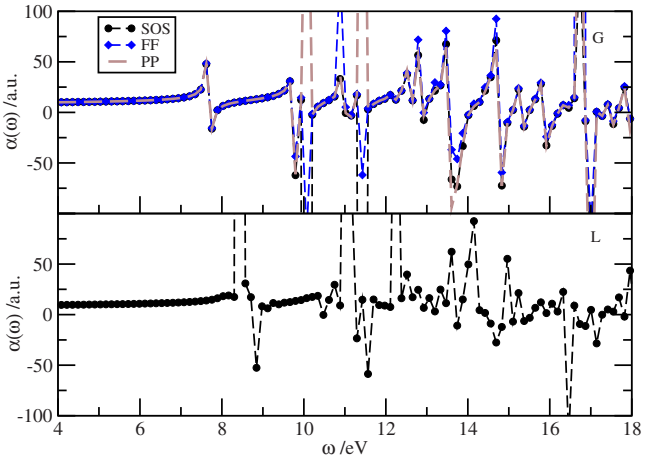

FIG. 2. (Color online) Comparison between SOS, PP, and FF calculations for the dynamic polarizability of the gas phase water molecule (top panel) and dynamic polarizability of liquid water $N_w=1+100$ (bottom panel) calculated with SOS.

corresponding to diverging values (poles of the real dynamic polarizability) are coincident. The fact that there is no truncation of the number of excited states in the PP approach should be emphasized.[52] Comparison between the top and bottom panels shows that, using the SOS procedure, the first pole of $\alpha(\omega)$ in the liquid is blueshifted by ~0.9 eV compared to the gas phase.

The low-energy behavior for the real part of the dynamic polarizability of the water molecule has been investigated by experimental[55] and theoretical studies.[46,47] This behavior is illustrated in Fig. 3 for water in the liquid and gas phases. Fitting of $\alpha(\omega)$ of expression (3) in the range of 0–2.7 eV leads to the Cauchy coefficients $S(-2)$, $S(-4)$, and $S(-6)$ reported in Table II. We will first discuss the gas phase results. BHandHLYP predictions for $S(-2)$ are 0.40 a.u. lower than the experimental value (9.64 a.u.).[55,56] PBE0 slightly overestimates $S(-2)$. Similar trends can be observed when we compare TDDFT predictions and experimental data for $S(-4)$ and $S(-6)$. EOM-CCSD results for $S(-2)$ are basis-set dependent. $S(-2)$ is 8.62 a.u. (dapvdz) and 9.24 a.u. (dapvtz). This last value is very similar to the BHandHLYP prediction, whereas the first one underestimates the experimental value by 1.02 a.u. However, it should be observed that vibrational contributions to the molecular polarizability[57] are not included in the present calculations. For the water molecule in vacuum this contribution is estimated as ~4% of the total polarizability.[57] If such a correction is added to our best estimates (EOM-CCSD and TDDFT-BHandHLYP with the dapvtz basis set) then $S(-2)$ would be ~9.6 a.u, which is in very good agreement with experiment.[55,56]

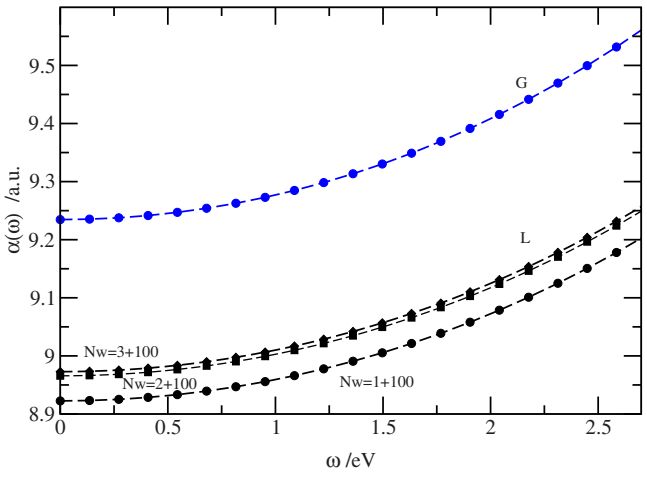

FIG. 3. (Color online) Low-energy behavior for the dynamic polarizability of water in the gas (G) and liquid (L) phases (BHandHLYP/dapvdz). Liquid phase calculations were performed for $N_w=1+100$ (circles), $N_w=2+100$ (squares), and $N_w=3+100$ (diamonds).

Cauchy coefficients for the liquid phase are also reported in Table II (values in parenthesis). All these liquid phase values are averaged over 100 configurations statistically uncorrelated sampled during the simulations (saved every 20 ps). TDDFT calculations indicate that the static polarizability of the water molecule in the liquid is ~4% lower than its gas phase values. This trend is also corroborated by EOM-CCSD calculations and it is in agreement with other theoretical results.[58] TDDFT predicts that $S(-4)$ in liquid water is ~14%–17% lower than its gas phase value, whereas $S(-6)$ is smaller by ~40% in the liquid. Experimental Cauchy coefficients for liquid water are apparently not available. The behavior of $\alpha(\omega)$ in the liquid phase for quantum systems with one, two, or three water molecules embedded in the charge distribution of other 100 water molecules is also shown in Fig. 3. The results indicate that in comparison with $N_w=2+100$ and $N_w=3+100$, $\alpha(w)$ for $N_w=1+100$ is vertically shifted by ~−0.04 a.u.. No significant differences are observed between the curves for $N_w=2+100$ and $N_w=3+100$.

B. Optical absorption spectrum of liquid water

In condensed phases, the relationship between the dielectric constant $\epsilon(\omega)=\epsilon_1(\omega)+i\epsilon_2(\omega)$ at high frequency and the dynamic polarizability $\alpha(\omega)$ is given by the Lorenz–Lorentz equation,[59]

$$\frac{\epsilon(\omega)-1}{\epsilon(\omega)+2}=\frac{4\pi}{3}\rho\alpha(\omega), \tag{4}$$

where the number density $\rho=N/V$, N is the number of particles and V is its volume. Before a comparison between theoretical results and experiment on the water absorption spectrum is presented, it is important to discuss how the results depend on the adopted theoretical approaches (EOM-CCSD and TDDFT-BHandHLYP), different basis sets (dapvxz; $x=D,T,Q$), number of states in the SOS (N_{states}), and on the number of water molecules explicitly included in the quantum system embedded in the charge distribution of more than 100 water molecules with the NCC model ($N_w=1+100$, $2+100$, $3+100$).

Calculations were also carried with two other different charge embeddings. In the first, the embedding charges are those of the TIP3P model for liquid water.[60] In the second one, atomic charges fitted to the electrostatic potential[61] for a quantum system of six water molecules embedded in the NCC charges of 100 water molecules were estimated at the BHandHLYP/dapvdz level. Then, calculations of electronic

TABLE II. Cauchy moments (a.u.) for the water molecule in the gas and liquid phase (values in parentheses). The Cauchy moments were fitted in the energy interval [0, 2.7] eV. The calculations were carried out with the NCC geometry for the water molecule.

		$S(-2)$	$S(-4)$	$S(-6)$
BHandHLYP	dapvdz	9.24(8.92)	31.02(27.0)	216.05(155.4)
		(8.96,[a]8.97[b])	(27.2,[a]27.2[b])	(157.1,[a]158.0[b])
	dapvtz	9.23(8.92)	30.87(26.84)	215.0(155.1)
	dapvqz	9.23(8.84)	30.82(26.72)	213.6(155.1)
PBE0	dapvtz	9.75(9.38)	36.92(31.48)	309.8(212.48)
EOM-CCSD	dapvdz	8.62(8.53)	35.26(30.46)	275.31(192.88)
	dapvtz	9.24	34.01	248.29
Expt.		9.64[c,d]	35.42[d]	240.1[d]

[a] $N_w=2$.
[b] $N_w=3$.
[c] From Ref. 56.
[d] From Ref. 55.

properties for a system with one quantum molecule surrounded by the self-consistent charges (SCF) of the nearest five water molecules embedded in 100 NCC charges [$N_w=1+5(\mathrm{SCF})+100(\mathrm{NCC})$] were calculated at the same theoretical level. The purpose of the second embedding was to assess how the self-consistent calculation of polarization effects for both the quantum system and the nearest five water molecules may affect the results in comparison with a frozen embedding. The results of these calculations are reported in Fig. 4 for TIP3P (top panel) and SCF (middle panel) embeddings. A small redshift (less than 0.1 eV) of the peak positions is observed for the SCF charges in comparison with the NCC frozen embedding. In agreement with Brancato *et al.*,[23] we confirmed that the results for the dielectric properties are not significantly dependent on the choice of the embedding charges. Therefore, it seems reasonable to dismiss the choice of embedding charges as a significant source of error in the prediction of the dielectric properties. This should be verified for interaction models that describe, at least approximately, polarization effects in the liquid phase. However, we should stress the interest of adopting a polarizable model for the embedding charges and to take into account in a self-consistent way the polarization of both the quantum system and embedding charges.[16]

Figure 4 (bottom panel) shows the imaginary part of the dielectric constant $\epsilon_2(\omega)$ for liquid water ($N_w=1+100$) predicted by EOM-CCSD and TDDFT calculations with the dapvdz basis set. A good agreement between the two approaches can be observed and the most significant difference between EOM-CCSD and TDDFT concerns the first maximum of $\epsilon_2(\omega)$, which is ~0.3 eV blueshifted by TDDFT. The middle panel of Fig. 4 also shows the basis-set dependence of the TDDFT results and it appears that $\epsilon_2(\omega)$ is not significantly dependent on the basis set (dapvdz, dapvtz, or dapvqz) for energies below 15 eV. Consequently, it seems reasonable to assume that by using the dapvdz basis set, the results for $\epsilon_2(\omega)$ based on EOM-CCSD and BHandHLYP are reliable below 15 eV. On the other hand, results for the absorption spectrum based on TDDFT for higher energies (up to 18 eV) should rely on calculations with the dapvqz basis set (see Fig. 4).

The dependence of $\epsilon_2(\omega)$ on the number of states in the SOS is illustrated in Fig. 5 (bottom) using TDDFT-BHandHLYP with the dapvdz basis set. Comparison between the results for $N_{\mathrm{states}}=120$ and 265 indicates that $\epsilon_2(\omega)$ is essentially unchanged by using a small number of states in the SOS and the positions of the maxima are not modified. This feature suggests that calculations for the dielectric properties with a larger number of particles in the quantum system could be carried out by using a smaller number of states. However, in any case, the convergence of the dynamic polarizability with the basis set and N_{states} should be checked.

Figure 5 (top panel) shows the behavior of $\epsilon_2(\omega)$ for quantum systems with 1–5 water molecules. These results were based on calculations with a smaller basis set and strongly suggest that no significant dependence of $\epsilon_2(\omega)$ on the size of the quantum system is observed when $N_w>3$. However, as previously discussed (see Table I and Fig. 4) at least a dapvdz basis set is necessary for reliable predictions of excitation energies. Therefore, accurate averaged proper-

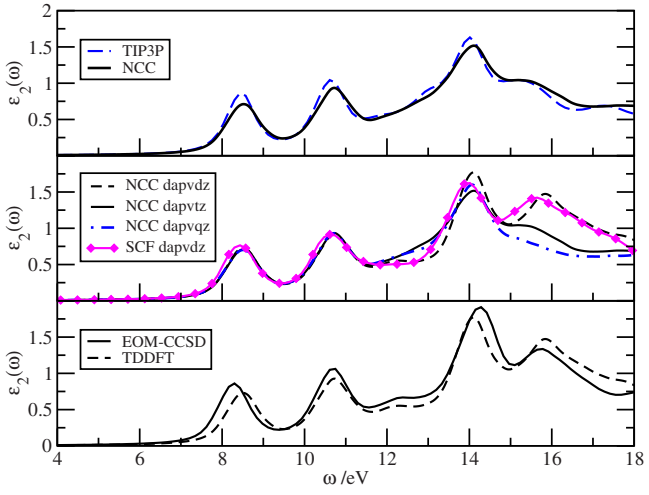

FIG. 4. (Color online) Imaginary part of the dielectric constant of liquid water ($\epsilon_2(\omega)$) for $N_w=1+100$. Top: comparison between TIP3P and NCC charge embedding with the dapvtz basis set. Middle: behavior of $\epsilon_2(\omega)$ using TDDFT-BHandHLYP with different basis sets (dapvdz, dapvtz, and dapvqz) in the 6–18 eV range and comparison between $\epsilon_2(\omega)$ calculated with the NCC frozen embedding and self-consistent charges (SCF). See text for details. Bottom: comparison between EOM-CCSD and TDDFT-BHandHLYP with the dapvdz basis set.

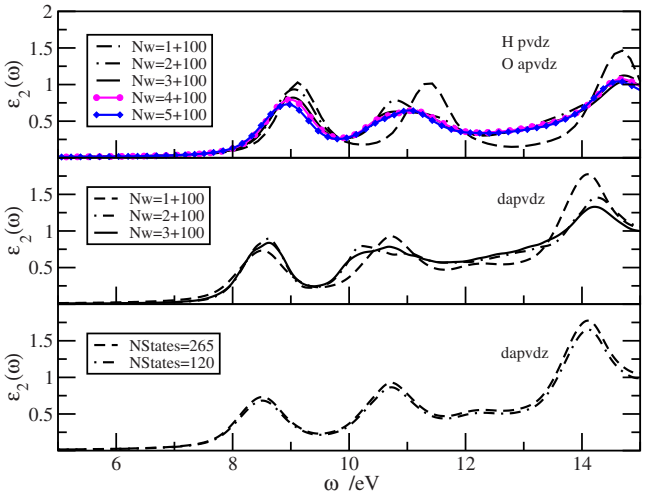

FIG. 5. (Color online) Dependence of $\epsilon_2(\omega)$ on the number of molecules in the quantum system and number of states included in the SOS from TDDFT-BHandHLYP calculations. Top: results for $N_w=(1-5)+100$ with the cc-pVDZ (H) and aug-cc-pVDZ (O) basis sets. Middle: results for $N_w=(1-3)+100$ with the dapvdz basis set. Bottom: dependence of $\epsilon_2(\omega)$ on the number of states included in the SOS (dapvdz).

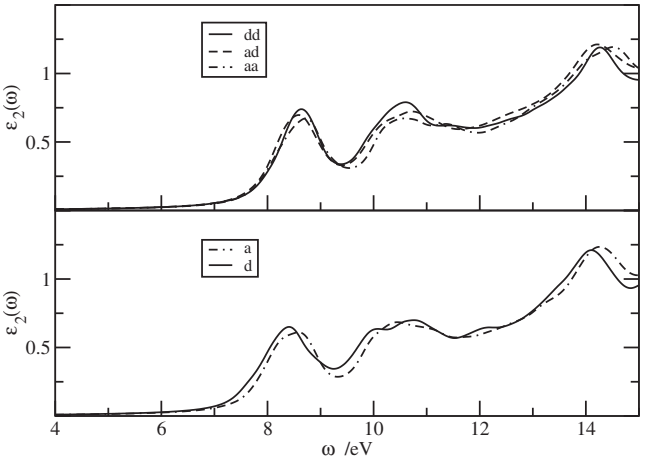

FIG. 6. Dependence of $\epsilon_2(\omega)$ on the number of hydrogen bonds for $N_w=3+100$ (BHandHLYP/dapvdz). The central water can form one (a;d) or two (aa;ad;dd) H-bonds with the other two water molecules in the quantum system.

ties (over 100 uncorrelated configurations) with larger basis sets will rely on quantum systems including explicitly a maximum of three water molecules. For calculations with the dapvdz basis set, the dependence of $\epsilon_2(\omega)$ on the number of water molecules included in the quantum system for $N_w=1+100$, $N_w=2+100$, and $N_w=3+100$ is also illustrated in Fig. 5 (middle panel). In comparison with $N_w=1+100$, the second band of $\epsilon_2(\omega)$ is broadened and redshifted by ~ 0.2 eV when $N_w=2+100$ and $N_w=3+100$. The broadening of $\epsilon_2(\omega)$ reflects electronic and thermal broadenings.[62,63] Electronic broadening is related to the size of the quantum system and number of excitations included in the SOS, whereas thermal broadening depends on the number of configurations. The similarity between the curves for $N_w=2+100$ and $N_w=3+100$ is an indication that a correct description of the water dielectric properties is possible by performing calculations for a small quantum system embedded in the polarization field of the liquid. However, the reliability of this approach is based on averaging over a significant number of uncorrelated configurations and by the inclusion of a large number of excited states in the SOS.

The absorption spectrum of liquid water will now be related with the local structure of the hydrogen (H) bond network. For $N_w=3+100$, we calculated the number of H-bonds that the central water makes with the two other molecules of the quantum system. The criterion for H-bond formation was that the O–O distance should be less than 3.5 Å and the O–H…O angle less than 35°. A given water molecule can accept (a) or donate (d) a hydrogen atom. For each configuration with three water molecules, the central molecule can form zero, one (a;d), or two (aa;ad;dd) H-bonds with the other two molecules in the quantum system. The fraction of the configurations for each case are the following: a(0.12), d(0.6), aa(0.13), ad(0.56), and dd(0.12). The behavior of $\epsilon_2(\omega)$, averaged over the configurations for the different cases is illustrated in Fig. 6. For configurations of type (a), where the central water molecules make only one H-bond as H-bond acceptor, $\epsilon_2(\omega)$ is blueshifted in comparison with configurations of type (d). The top panel of Fig. 6 shows $\epsilon_2(\omega)$ for configurations with two H-bonds. In this case, no significant difference in the first maximum position of $\epsilon_2(\omega)$ is observed. However, the second band for (aa) configurations is blueshifted although the second maximum positions are nearly the same for (aa) and (ad) configurations. The blueshift of $\epsilon_2(\omega)$ for (aa) configurations is possibly related to the energetic stabilization of the quantum system when the H-bond interaction involves directly the oxygen atom of the central molecule. Therefore, for $N_w=3+100$ the broadening of the $\epsilon_2(\omega)$ second band can be possibly explained by differences between the electronic excitation energies of (dd) and (aa) configurations.

Dielectric properties of water in the gas and liquid phases based on TDDFT calculations are reported in Fig. 7, where $\epsilon_1(\omega)$, $\epsilon_2(\omega)$, as well as the energy loss function $[-\mathrm{Im}(1/\epsilon)]$ are represented. The most significant feature characterizing the dielectric behavior of liquid water is that the two first maxima of $\epsilon_2(\omega)$ are blueshifted by ~ 0.9 eV relative to their gas phase values. This first maximum is as-

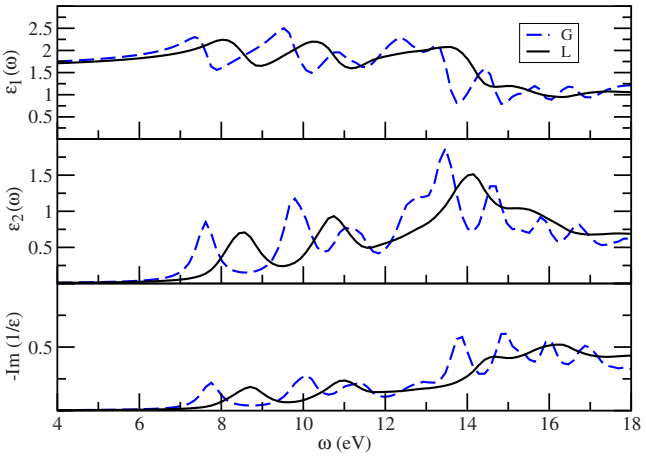

FIG. 7. (Color online) Comparison between dielectric properties of water in the gas (G) and liquid (L) phases ($N_w=1+100$ and BHandHLYP/dapvqz).

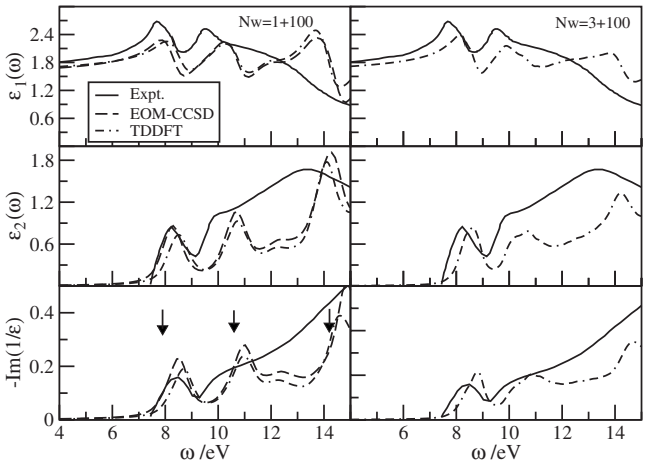

FIG. 8. Comparison between theoretical predictions (EOM-CCSD and TDDFT with the dapvdz basis set) and experimental data for the dielectric properties of liquid water. Vertical arrows indicate the maxima for the reflectance spectrum of liquid water reported by Hayashi *et al.* (Ref. 10).

sociated with the gas phase $1\ ^1B_1 \leftarrow 1X\ ^1A_1$ transition and its gas to liquid blueshift agrees well with the experimental value (0.96 eV).[8] However, the first maximum position of $\epsilon_2(\omega)$ predicted by BHandHLYP (8.5 eV) is displaced to higher energies by 0.3 eV in comparison with the maximum in the optical conductivity of water (8.2 eV).[5] Similar shifts (~0.9 eV) to higher energies are also observed when we compare gas and liquid phase predictions for $\epsilon_1(\omega)$ and $[-\mathrm{Im}(1/\epsilon)]$.

Experimental data for the dielectric properties of liquid water indicate that $\epsilon_2(\omega)$ is characterized by three broad bands with maxima approximately at 8.2, 10.0, and 13.7 eV.[5] More recently, Hayashi *et al.*[10] pointed out some discrepancies between the curves for the reflectance of liquid water obtained by inelastic x-ray scattering spectroscopy and the data of Heller *et al.*[5] The differences mainly concern results for energies above 15 eV and, although the positions of the first maximum coincide (~7.9 eV), the positions of the second and third maxima reported by Hayashi *et al.*[10] are apparently blueshifted by ~0.6 eV relative to the data of Heller *et al.*[5] (see Fig. 3 of Ref. 10).

Data for the dielectric properties of liquid water are reported in Fig. 8, where EOM-CCSD and TDDFT-BHandHLYP results are compared with data from Heller *et al.*[5] for $\epsilon_1(\omega)$, $\epsilon_2(\omega)$, and $[-\mathrm{Im}(1/\epsilon)]$. Regarding the results with $N_w=1+100$ (left panel of Fig. 8) some aspects are worth remarking. First, a very good agreement between the EOM-CCSD results and experiment for the first maximum position is observed for all of the three curves. However, the EOM-CCSD results for $\epsilon_2(\omega)$ indicate that the positions of the second (10.7 eV) and third (14.2 eV) maxima are blueshifted by ~0.7 eV in comparison with the results of Heller *et al.*[5] EOM-CCSD and TDDFT calculations predict similar positions for the second and third maxima of $\epsilon_1(\omega)$ and $\epsilon_2(\omega)$. The first maximum of $\epsilon_2(\omega)$ predicted by TDDFT is blueshifted by ~0.3 eV relative to the experimental data of Heller *et al.*,[5] whereas the positions of the second (10.7 eV) and third (14.1 eV) maxima are also blueshifted in comparison with experiment.[5] The results for $N_w=3+100$ (right panel of Fig. 8) indicate that the broadening of the $\epsilon_2(\omega)$ second band that was previously discussed seems to improve the agreement with experiment, particularly in the case of the energy loss function $[-\mathrm{Im}(1/\epsilon)]$.

The vertical arrows in the lower panel of Fig. 8 for $N_w=1+100$ indicate the positions of the three first maxima (7.9, 10.6, and 14.2 eV) for the reflectance of liquid water from the data of Hayashi *et al.*[10] If it is assumed that the 0.6 eV blueshift in the reflectance of Hayashi *et al.*[10] for the positions of the second and third maxima will induce a similar shift on $\epsilon_1(\omega)$, $\epsilon_2(\omega)$, and $[-\mathrm{Im}(1/\epsilon)]$, then, the agreement between our results (particularly those based on EOM-CCSD calculations) and experimental information is significantly improved. Our theoretical study thus suggests that the more recent experimental data of Hayashi *et al.*[10] apparently provide a better description of the high-energy side of the liquid water absorption spectrum.

IV. CONCLUSIONS

Sequential MD/QM results for the dynamic polarizability, Cauchy coefficients, and dielectric properties of liquid water were reported. The MD simulations were based on a polarizable model for liquid water. 100 uncorrelated MD configurations were then used in the QM calculations, which were based on TDDFT-BHandHLYP and EOM-CCSD methods. Initially, we verified that excitation energies for the isolated water molecule predicted by the two adopted theoretical approaches were in very good agreement between them and also with experiment. Moreover, the dynamic polarizabilities of the gas phase water molecule predicted by SOS and FF procedures are quite similar. A reliable prediction of the dielectric properties of water can be carried out in the 6–15 eV energy range with a dapvdz basis set. However, for higher energies, improved basis sets are needed. Our calculations indicate that Cauchy coefficients for liquid water are smaller than those for the isolated water molecule, which reflects modifications of the low-energy range optical properties of liquid water in comparison with the gas phase regime.

We analyzed the dependence of the results for the imaginary part of the dielectric constant ($\epsilon_2(\omega)$) on the number of water molecules explicitly included in the quantum system. It was concluded that its behavior was correctly described by carrying out calculations with a single water molecule in the quantum system. However, the explicit inclusion of a larger number of molecules leads to a broadening of the second band of $\epsilon_2(\omega)$. For a quantum system with three water molecules, we discussed how the absorption spectrum depends on HB. Our results confirm that the acceptor/donor character and the number of H-bonds may significantly affect $\epsilon_2(\omega)$.

A very good agreement between EOM-CCSD calculations and the experimental data from Heller *et al.*[5] is obtained for the first maximum of $\epsilon_2(\omega)$. However, some distinctions were noted for the positions of the second and third maxima. The agreement with experiment is apparently improved when the number of water molecules in the quantum system increases or when comparison is made with more recent experimental information.[10]

ACKNOWLEDGMENTS

This work was partially supported by a FCT (Portugal)/CAPES (Brazil) bilateral agreement. R.A.M. gratefully acknowledges the FCT (Portugal) (Grant No. SFRH/BPD/38447/2007). B.J.C.C. acknowledges support from Fundação para a Ciência e a Tecnologia (FCT), Portugal (Grant Nos. POCI/MAT/55977/2004 and PTDC/QUI/68226/2006). K.C. and S.C. acknowledge continuous support from CNPq and FAPESP.

[1] R. E. Verrall and W. A. Senior, J. Chem. Phys. **50**, 2746 (1969).
[2] D. Yeager, V. McKoy, and G. A. Segal, J. Chem. Phys. **61**, 755 (1974).
[3] E. N. Lassettre and E. R. White, J. Chem. Phys. **60**, 2460 (1974).
[4] W. T. Murphy, J. Chem. Phys. **67**, 5877 (1977).
[5] J. M. Heller, Jr., R. N. Hamm, R. D. Birkhoff, and L. R. Painter, J. Chem. Phys. **60**, 3483 (1974).
[6] J. M. Heller, Jr., R. D. Birkhoff, and L. R. Painter, J. Chem. Phys. **67**, 1858 (1977).
[7] K. H. Tan, C. E. Brion, Ph. E. Van der Leeuw, and M. J. Van der Wiel, Chem. Phys. **29**, 299 (1978).
[8] T. I. Quickenden and J. A. Irvin, J. Chem. Phys. **72**, 4416 (1980).
[9] W. F. Chan, G. Cooper, and C. E. Brion, Chem. Phys. **178**, 387 (1993).
[10] H. Hayashi, N. Watanabe, Y. Udagawa, and C.-C. Kao, J. Chem. Phys. **108**, 823 (1998).
[11] R. R. Dagastine, D. C. Prieve, and L. R. White, J. Colloid Interface Sci. **231**, 351 (2000).
[12] T. W. Marin, K. Takahashi, and D. M. Bartels, J. Chem. Phys. **125**, 104314 (2006).
[13] B. Bagchi, Chem. Rev. **105**, 3197 (2005).
[14] N. W. Winter, W. A. Goddard III, and F. W. Borowicz, J. Chem. Phys. **62**, 4325 (1975).
[15] O. Christiansen, T. M. Nymand, and K. V. Mikkelsen, J. Chem. Phys. **113**, 8101 (2000).
[16] J. Kongsted, A. Oested, K. V. Mikkelsen, and O. Christiansen, J. Chem. Phys. **118**, 1620 (2003).
[17] J. Kongsted, A. Osted, K. V. Mikkelsen, and O. Christiansen, J. Chem. Phys. **119**, 10519 (2003).
[18] A. Osted, J. Kongsted, K. V. Mikkelsen, P.-O. Åstrand, and O. Christiansen, J. Chem. Phys. **124**, 124503 (2006).
[19] M. Yang, P. Senet, and C. Van Alsenoy, Int. J. Quantum Chem. **101**, 535 (2005).
[20] C. R. Jacob, J. Neugebauer, L. Jensen, and L. Visscher, Phys. Chem. Chem. Phys. **8**, 2349 (2006).
[21] P. H. Hahn, W. G. Schmidt, K. Seino, M. Preuss, F. Bechstedt, and J. Bernholc, Phys. Rev. Lett. **94**, 037404 (2005).
[22] V. Garbuio, M. Cascella, L. Reining, R. Del Sole, and O. Pulci, Phys. Rev. Lett. **97**, 137402 (2006).
[23] G. Brancato, N. Rega, and V. Barone, Phys. Rev. Lett. **100**, 107401 (2008).
[24] D. Lu, F. Gygi, and G. Galli, Phys. Rev. Lett. **100**, 147601 (2008).
[25] S. Senapati and A. Chandra, J. Phys. Chem. B **105**, 5106 (2001).
[26] J. Martí, G. Nagy, E. Guàrdia, and M. C. Gordillo, J. Phys. Chem. B **110**, 23987 (2006).
[27] H. Weingartner and E. U. Franck, Angew. Chem. Int. Ed. **44**, 2672 (2005).
[28] U. Niesar, G. Corongiu, E. Clementi, G. R. Kneller, and D. K. Bhattacharya, J. Phys. Chem. **94**, 7949 (1990).
[29] M. A. L. Marques and E. K. U. Gross, in *A Primer in Density Functional Theory*, edited by C. Fiolhais, F. Nogueira, and M. Marques (Springer, Berlin, 2002), Chap. 4.
[30] J. F. Stanton and R. J. Bartlett, J. Chem. Phys. **98**, 7029 (1993).
[31] C. Millot and B. J. C. Cabral, Chem. Phys. Lett. **460**, 466 (2008).
[32] A. K. Soper and R. N. Silver, Phys. Rev. Lett. **49**, 471 (1982).
[33] A. K. Soper, F. Bruni, and M. A. Ricci, J. Chem. Phys. **106**, 247 (1997).
[34] G. Hura, J. M. Sorensen, R. M. Glaeser, and T. M. Head-Gordon, J. Chem. Phys. **113**, 9140 (2000).
[35] J.-C. Soetens, M. T. C. M. Costa, and C. Millot, Mol. Phys. **94**, 577 (1998).
[36] K. Coutinho and S. Canuto, Adv. Quantum Chem. **28**, 89 (1997).
[37] A. D. Becke, Phys. Rev. A **38**, 3098 (1988).
[38] C. Lee, W. Yang, and R. G. Parr, Phys. Rev. B **37**, 785 (1988).
[39] M. J. Frisch G. W. Trucks, H. B. Schlegel *et al.*, GAUSSIAN-03, Rev. C.02 Gaussian Inc., Pittsburgh, PA, 2003.
[40] C. Adamo and V. Barone, J. Chem. Phys. **110**, 6158 (1999).
[41] J. P. Perdew, K. Burke, and M. Ernzerhof, Phys. Rev. Lett. **77**, 3865 (1996).
[42] H.-J. Werner, P. J. Knowles, R. Lindh *et al.*, MOLPRO, version 2006.4, a package of *ab initio* programs, see http://www.molpro.net.
[43] D. E. Woon and T. H. Dunning, Jr., J. Chem. Phys. **98**, 1358 (1993).
[44] D. Ayma, J. P. Campillo, M. Rérat, and M. Causà, J. Comput. Chem. **18**, 1253 (1997).
[45] A. Naves de Brito, R. Feifel, A. Mocelin, A. B. Machado, S. Sundin, I. Hjelte, S. L. Sorensen, and O. Björneholm, Chem. Phys. Lett. **309**, 377 (1999).
[46] C. Hättig, G. Jansen, B. A. Hess, and J. G. Angyàn, Can. J. Chem. **74**, 976 (1996).
[47] C. Van Caillie and R. D. Amos, Chem. Phys. Lett. **328**, 446 (2000).
[48] Z.-L. Cai, D. J. Tozer, and J. R. Reimers, J. Chem. Phys. **113**, 7084 (2000).
[49] L. Lee and M. Suto, Chem. Phys. **110**, 161 (1986).
[50] T. Yanai, D. P. Tew, and N. C. Handy, Chem. Phys. Lett. **393**, 51 (2004).
[51] M. J. Paterson, O. Christiansen, F. Pawłowski, P. Jørgensen, C. Hättig, T. Helgaker, and P. Sałek, J. Chem. Phys. **124**, 054322 (2006).
[52] P. Norman, D. M. Bishop, H. J. Aa, and J. Oddershede, J. Chem. Phys. **115**, 10323 (2001).
[53] U. Ekström, P. Norman, V. Caravetta, and H. Ägren, Phys. Rev. Lett. **97**, 143001 (2006).
[54] T. Helgaker, H. J. Aa. Jensen, and P. Jørgensen *et al.*, DALTON, an *ab initio* electronic structure program, release 2.0, 2005, see http://www.kjemi.uio.no/software/dalton.html.
[55] G. D. Zeiss and W. J. Meath, Mol. Phys. **33**, 1155 (1977).
[56] M. A. Spackman, J. Phys. Chem. **93**, 7594 (1989).
[57] P. K. K. Pandey and D. P. Santry, J. Chem. Phys. **73**, 2899 (1980).
[58] A. Morita, J. Comput. Chem. **23**, 1466 (2002).
[59] C. J. F. Bøttcher, *Theory of Electric Polarization* (Elsevier, Amsterdam, 1973).
[60] W. L. Jorgensen, J. D. Madura, R. W. Impey, and M. L. Klein, J. Chem. Phys. **79**, 926 (1983).
[61] C. M. Breneman and K. Wiberg, J. Comput. Chem. **11**, 361 (1990).
[62] P. Hunt, M. Sprik, and R. Vuilleumier, Chem. Phys. Lett. **376**, 68 (2003).
[63] P. C. do Couto, B. J. C. Cabral, and S. Canuto, Chem. Phys. Lett. **429**, 129 (2006).